

# Study on Arterial Tissue Characterization with Ultrasound

Hideyuki Hasegawa<sup>1,2</sup> and Hiroshi Kanai<sup>2,1</sup>

1 Graduate School of Biomedical Engineering, Tohoku University

2 Graduate School of Engineering, Tohoku University

E-mail: [hasegawa@ecei.tohoku.ac.jp](mailto:hasegawa@ecei.tohoku.ac.jp), [hkanai@ecei.tohoku.ac.jp](mailto:hkanai@ecei.tohoku.ac.jp)



## Abstract

The endothelial dysfunction is considered to be an initial step in atherosclerosis. Additionally, it was reported that the smooth muscle, which constructs the media of the artery, changes its characteristics owing to atherosclerosis. Therefore, it is essential to develop a method of assessing the regional endothelial function and mechanical properties of the arterial wall. To evaluate the endothelial function, a conventional technique of measuring the transient change in the diameter of the brachial artery caused by flow-mediated dilation (FMD) after the release of avascularization is used. However, this method cannot evaluate the mechanical properties of the wall. We previously developed a method for the simultaneous measurements of waveforms of radial strain and blood pressure in the radial artery. In this study, the viscoelasticity of the arterial wall was estimated from the measured stress-strain relationship using the least-squares method and the transient changes in the mechanical properties of the arterial wall were revealed. From *in vivo* experimental results, the stress-strain relationship showed a hysteresis loop and viscoelasticity was estimated by the proposed method. The slope of the loop decreased owing to FMD, which resulted in the decrease in estimated elastic modulus. The increase in the area of the loop occurred after recirculation, which corresponds to the increase in the ratio of the loss modulus (depends on viscosity) to the elastic modulus when the Voigt model is assumed. In this study, the variance in estimates was evaluated by *in vivo* measurement for 10 min. The temporal decrease in static elasticity after recirculation due to FMD was much larger than the evaluated variance. These results show a potential of the proposed method for the thorough analysis of the transient change in viscoelasticity due to FMD.

In addition to the mechanical property and function of the arterial wall, the condition of blood, such as red blood cell (RBC) aggregation, a determinant of blood viscosity, plays an important role in blood flow rheology. RBC aggregation is induced by the adhesion of RBCs when the electrostatic repulsion between RBCs weakens owing to increases in protein and saturated fatty acid levels in blood, and excessive RBC aggregation may lead to various circulatory diseases. This study was conducted to establish a noninvasive

quantitative method for the assessment of RBC aggregation. The spectrum of nonaggregating RBCs presents Rayleigh behavior, indicating that the power of a scattered wave is proportional to the fourth power of frequency. By dividing the measured power spectrum of echoes from scatterers by that from a silicone plate reflector, the frequency responses of transmitting and receiving transducers are removed from the former spectrum. This normalized power spectrum changes linearly with respect to logarithmic frequency. In non-Rayleigh scattering, on the other hand, the spectral slope decreases because a larger scatterer behaves as a reflector and echoes from a reflector do not show frequency dependence. Therefore, it is possible to assess RBC aggregation using the spectral slope value. In this study, spherical scatterers with diameters of 5, 11, 15, and 30  $\mu\text{m}$  were measured in basic experiments. The spectral slope of the normalized power spectrum of echoes from the lumen of the vein in the dorsum manus of a 24-year-old healthy male was close to that from microspheres with a diameter of 15  $\mu\text{m}$ , and the typical RBC diameter was smaller than this value. The frequency-dependent attenuation of ultrasound during propagation in a biomedical tissue was considered to be one reason for this. Furthermore, during avascularization, the slope gradually decreased owing to the aggregation of RBCs. These results show the possibility of using the proposed method for the noninvasive assessment of RBC aggregation.

## 1. Introduction

### 1.1. Measurements of flow mediated dilation

The main cause of circulatory diseases is considered to be atherosclerosis. Therefore, the quantitative assessment of atherosclerosis is essential for making an early diagnosis of these diseases.

The endothelial dysfunction is considered to be an initial step in atherosclerosis [1]. Additionally, it was reported that the smooth muscle, which constructs the media of the artery, changes its characteristics owing to atherosclerosis [2]. Consequently, it is important for an early preventive treatment to noninvasively assess the endothelial function and mechanical properties of the media mainly composed of smooth muscle.

Endothelial cells react to the shear stress caused by blood flow and produce nitric oxide (NO), which is known as a vasodepressor material. The smooth muscle

is relaxed as a result of the response to the produced NO. This function is important for maintaining the homeostasis of the vascular system. Smooth muscle cells in the media are classified into two types with different functionalities [3]. The composite type is proliferative, and the contractional type contracts and relaxes as responses to chemical and mechanical stimuli.

When the blood vessel is initially formed, smooth muscle cells change their type from composite to contractional and control blood flow and blood pressure. On the other hand, after the vascular system is established, smooth muscle cells change their characteristics from contractional to composite owing to atherosclerosis. The composite type is related to the growth factor and accelerates the migration of smooth muscle cells to the intimal layer. Therefore, as described above, the evaluation of the endothelial function and characteristics of smooth muscle cells is important for the early diagnosis of atherosclerosis.

For the evaluation of the endothelial function, there is a conventional technique of measuring the transient change in the inner diameter of the brachial artery caused by flow-mediated dilation (FMD) after the release of avascularization [4]. For a more sensitive and regional evaluation, we developed a method of directly measuring the change in the elasticity of the intima-media region due to FMD [5].

We propose a method for the evaluation of FMD, which was previously applied to the measurement of the radial artery. There is an inversely proportional relationship between the percent change in inner diameter due to FMD and that in the inner diameter of the artery at rest because the flow velocity, which affects the shear stress, is inversely proportional to the square of the inner diameter when the pressure and flow volume are constant [6]. Additionally, the blood pressure (stress) waveform can be continuously measured in the radial artery, together with the minute change in thickness (radial strain), which is measured using the ultrasonic phased tracking method [7]. From such measurements, we could determine the stress-strain relationship during each heartbeat [8]. Therefore, the radial artery would be a more suitable site for the measurement of FMD.

In this study, from the stress-strain relationship during each heartbeat, the viscoelasticity of the intima-media region was estimated using the least-squares method, and the transient change in viscoelasticity due to FMD was estimated. In addition, the viscoelasticity at rest was measured for 10 min to evaluate the variance in measurements [9].

## 1.2. Evaluation of red blood cell aggregation

Medical ultrasound is clinically used to make a diagnosis for various organs, and because it is noninvasive and relatively stress free for patients, it can be repeatedly employed to confirm time-dependent changes. Ultrasound B-mode imaging is widely used for the morphological diagnosis of the arterial wall. In addition, methods for evaluating the viscoelasticity of the arterial wall have recently been developed [8,10]

because the mechanical properties of the arterial wall are related to the atherosclerotic change.

The condition of blood is an important factor related to various circulatory diseases. However, conventional ultrasonic images cannot be used to evaluate the condition of the blood in the blood vessel because red blood cells (RBCs), which are the main components of blood, are much smaller than the wavelength of ultrasound and the variation in acoustic impedance between blood plasma and RBCs is very small. However, the condition of blood is related to various circulatory diseases, and the evaluation and diagnosis of such a condition are important for the detection of a disease at an early stage.

As one of the determinants of blood viscosity, RBC aggregation plays an important role in blood flow rheology. The adventitia of healthy RBCs is charged with negative electricity, which impedes RBC adherence by electrostatic repulsion [11]. However, owing to increases in protein and saturated fatty acid levels in blood, such repulsion between RBCs is gradually weakened and RBC aggregation is induced by the overlapping of RBCs. The main function of blood is to transport nutrients, oxygen, and essential elements to tissues and to remove metabolic products, such as carbon dioxide and lactic acid, produced by those tissues [12]. However, RBC aggregation significantly degrades this function because of the decrease in the superficial area used to transport materials. Excessive RBC aggregation may promote various circulatory diseases, such as atherosclerosis, hypercholesterolemia, diabetes, thrombosis, and so on [13-16]. Therefore, the assessment of RBC aggregation is essential [17]. The micro channel array flow analyzer (MCFAN) method is a recently developed technique for the assessment of RBC aggregation by determining whether red blood cells pass through gaps in silicon substrates simulating blood capillaries [18]. However, this method is invasive and is not quantitative. The present study was conducted to establish a noninvasive quantitative method for the assessment of RBC aggregation [19].

## 2. Materials and Methods

### 2.1. Measurement of viscoelasticity of radial arterial wall

#### 2.1.1. Measurement of minute change in thickness of arterial wall for measurement of stress-strain relationship

The arterial wall is composed of three layers, namely, intima, media and adventitia. The smooth muscle, which constructs the media, is the main source of the viscoelasticity of the vessel wall. Therefore, the dilation and contraction of the artery depend on the characteristics of the media. The detailed analysis of the change in the viscoelasticity of the arterial wall due to FMD requires the *in vivo* measurement of the stress-strain relationship, which has not been measured noninvasively thus far.

The blood pressure waveform can only be measured noninvasively *in vivo* at the radial artery. However, it is impossible to measure the strain of the radial arterial wall by ultrasound at a typical frequency (10 MHz) in conventional equipment. Therefore, we constructed an acquisition system for high-frequency ultrasound [8]. This system improved the spatial resolution in the axial direction. Therefore, this system allows more detailed measurements and analyses. Figure 1 shows the B-mode images of the radial artery along the longitudinal axis and in the plane perpendicular to the axis of the artery.

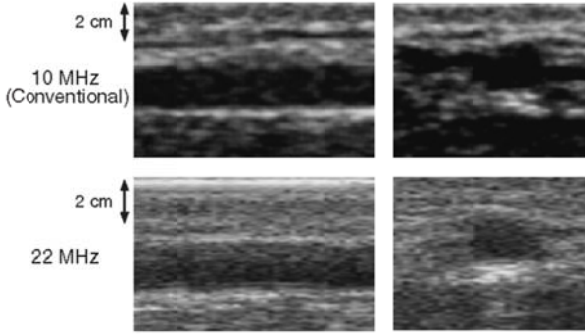


Fig. 1. B-mode images of the radial artery along the longitudinal axis (left) and in the plane perpendicular to the arterial longitudinal direction (right).

To determine the stress-strain relationship, the minute change in the thickness (strain)  $\Delta h(t)$  of the right radial arterial wall during a cardiac cycle was measured using the phased tracking method [7]. Together with the measurement of RF signals for the estimation of  $\Delta h(t)$ , the waveform of blood pressure (stress)  $p(t)$  in the left radial artery was continuously measured with a sphygmometer.

To obtain the change in thickness, the velocities of artery-wall boundaries (lumen-intima and media-adventitia) were estimated. The velocity  $v(t)$  was estimated from the phase shift  $\Delta\theta(t)$  of echoes in two consecutive frames. The phase shift  $\Delta\theta(t)$  was obtained using the complex cross-correlation applied to the demodulated signals of RF echoes. From the estimated phase shift  $\Delta\theta(t)$ , the average velocity  $\bar{v}(t)$  of the arterial wall at the pulse repetition interval  $T$  was obtained as

$$\hat{v}(t) = -\frac{c_0}{2\omega_0} \frac{\Delta\hat{\theta}(t)}{T}, \quad (1)$$

where  $\omega_0$  and  $c_0$  are the center angular frequency of the ultrasound wave and the speed of sound, respectively. The change in thickness,  $\Delta h(t)$ , between two different depths, A and B (corresponding to the boundaries of the arterial wall), in the arterial wall along an ultrasonic beam was obtained from the difference between displacements,  $x_A(t)$  and  $x_B(t)$ , at these two positions as

$$\begin{aligned} \Delta\hat{h}(t) &= \hat{x}_A(t) - \hat{x}_B(t) \\ &= \int_0^t [\hat{v}_A(t) - \hat{v}_B(t)] dt. \end{aligned} \quad (2)$$

The change in thickness,  $\Delta h(t)$ , corresponds to the incremental strain in the arterial radial direction at the time  $t$  due to the pressure increment  $\Delta p(t)$  from the diastolic pressure.

### 2.1.2. Estimation of viscoelasticity of arterial wall using least-squares method

The smooth muscle constructs the media and is the main source of the viscoelasticity of the arterial wall. We assumed a viscoelastic model as a mechanical model of the arterial wall to estimate its viscoelasticity.

There are many types of models for describing the viscoelasticity of the arterial wall. We selected a viscoelastic model with two components to simply understand the viscoelastic behavior of the arterial wall; one component corresponds to elasticity and the other to viscosity. In this study, the Voigt model was used because the deformation of the arterial wall during one cardiac cycle is reproducible among cardiac cycles, and there is no permanent deformation. The Maxwell model, which is another model with two components, was not used because it should be used for viscoelastic materials showing a permanent deformation.

By assuming the Voigt model as a viscoelastic model of the intima-media region, the stress-strain relationship is given by

$$\hat{\tau}(t) = E_s \gamma(t) + \eta \dot{\gamma}(t) + \tau_0, \quad (3)$$

where  $\hat{\tau}(t)$  is the stress modeled by the Voigt model and  $\gamma(t)$ ,  $\dot{\gamma}(t)$ ,  $E_s$ , and  $\eta$  are the strain, strain rate, static elasticity, and viscosity, respectively. In the *in vivo* measurement, the measured strain  $\gamma(t)$  is the incremental strain due to the pulse pressure, whereas the measured stress includes the bias stress (diastolic blood pressure). Therefore,  $\tau_0$  is added to the right-hand side of eq. (3) as the bias stress corresponding to diastolic pressure.

The parameters in eq. (3),  $E_s$ ,  $\eta$ , and  $\tau_0$  are estimated using the least-squares method by minimizing the mean squared error  $\alpha$  between the measured  $\tau(t)$  and model  $\hat{\tau}(t)$  stresses and defined by

$$\alpha = E_t [\{\tau(t) - \hat{\tau}(t)\}^2], \quad (4)$$

where  $E_t[\dots]$  indicates the averaging operation during a cardiac cycle. The parameters  $E_s$ ,  $\hat{\eta}$ , and  $\hat{\tau}_0$  that minimize  $\alpha$  are determined by setting the partial derivatives of  $\alpha$  with respect to  $E_s$ ,  $\eta$ , and  $\tau_0$  to zero as

$$\frac{\partial \alpha}{\partial E_s} = 0, \frac{\partial \alpha}{\partial \eta} = 0, \frac{\partial \alpha}{\partial \tau_0} = 0. \quad (5)$$

To solve the simultaneous equations, the optimum parameters that minimize  $\alpha$  are determined.

### 2.1.3. Procedure for *in vivo* measurement

The right radial arteries of two healthy male subjects (subject A: 35 years old and subject B: 22 years old) were measured. In these measurements, ultrasonic RF echoes (transmit: 22 MHz) were acquired at a sampling frequency of 66.5MHz for 2 s and the frame rate was about 160 Hz [8]. The acquisition for the evaluation of FMD was repeated every 20 s for 2 min at rest before avascularization and every 12 s for 3 min after recirculation. Together with the measurement of RF signals, the waveform of blood pressure  $p(t)$  in the left radial artery was continuously measured with a sphygmometer (Colin Jentow-7700). Additionally, for the evaluation of reproducibility, RF data and the blood pressure waveform at rest were measured every 1 min for 10 min. In this study, a sphygmometer, which automatically optimizes the position of the sensor for blood pressure measurement by detecting the regional pulsation of the radial artery, was used for the continuous measurement of the blood pressure waveform  $p(t)$  for about 10 min. However, the sphygmometer always requires the arterial pulsation to optimize the position of the sensor. In this measurement, therefore, the sensor of the sphygmometer was placed in the left arm, in which avascularization was not induced.

The experimental apparatus employed in this study showed undesirable time delays. We corrected the time delay between stress and strain to determine the stress-strain relationship that depended on only the viscoelasticity of the arterial wall [8]. The transient change in stress-strain relationship during a cardiac cycle due to FMD was obtained from the measured change in the thickness  $\Delta h(t)$  of the arterial wall and from the blood pressure  $\Delta p(t)$ .

### 2.2. Evaluation of red blood cell aggregation

An RBC is a very small ultrasonic scatterer whose diameter is 8  $\mu\text{m}$  at most, and thus, the amplitudes of scattered RF echoes are very small. To assess the level of RBC aggregation, the power spectrum of the echoes from RBCs is calculated using the fast Fourier transform (FFT), and the scattering properties of RF echoes are evaluated in the frequency domain. In the present study, it was assumed that the diameter of a scatterer increases depending on the degree of RBC aggregation.

The scattering strength can be measured quantitatively in terms of a backscattering coefficient if the tissues can be modeled as a random medium. Figure 2 shows the geometrical condition in the measurement of echoes from a random medium with a circular transducer [20]. The average power spectrum  $S_i(f)$  of incoherent components of the echo scattered by the random medium is given by

$$S_i(f) = |4\pi f \rho_0 G(f)|^2 k^4 R_s^2 g(f) \left(\frac{S_0}{2\pi w_0}\right)^4, \quad (6)$$

where  $k$  is the wave number of ultrasonic waves ( $k = 2\pi f / c_0$ ,  $c_0$  is the average sound velocity),  $\rho_0$  is the average density of the medium,  $G(f)$  is the electric characteristic of the transducer,  $R_s$  is the standard deviation of the amplitude reflection coefficients of scatterers,  $S_0$  is the area of the transducer aperture, and  $w_0$  is the distance between the transducer and the scatterers. Furthermore,  $g(f)$  is expressed as

$$g(f) = \left(\frac{\pi^{2.5} \sigma_b^2 d \sigma}{4}\right) (\sigma_b^{-2} + \sigma_T^{-2} + \sigma^{-2})^{-1} e^{-\sigma^2 k^2}, \quad (7)$$

where  $d$  is the thickness of the layer of the medium including scatterers,  $\sigma_b$  and  $\sigma_T$  are the beam radius ( $\sigma_b = 8^{0.5} w_0 / ka$ ) and  $a/2^{0.5}$  ( $a$ : aperture radius), respectively, and  $\sigma$  is the correlation length of continuous inhomogeneous media [21], being related to the diameter of the scatterer [20]. In this case, the correlation length is much smaller than the diameter and beam width of the transducer. Therefore, the following approximation holds:

$$(\sigma_b^{-2} + \sigma_T^{-2} + \sigma^{-2})^{-1} = \left\{ \sigma^{-2} \left[ \left(\frac{\sigma_b}{\sigma}\right)^{-2} + \left(\frac{\sigma_T}{\sigma}\right)^{-2} + 1 \right] \right\}^{-1} \cong \sigma^2. \quad (8)$$

Using eq. (8), eq. (6) is modified as

$$S_i(f) = |G(f)|^2 Z_0^2 R_s^2 d \left(\frac{a^6}{w_0^2}\right) \left(\frac{\pi^{2.5} k^4 \sigma^3 e^{-k^2 \sigma^2}}{2}\right), \quad (9)$$

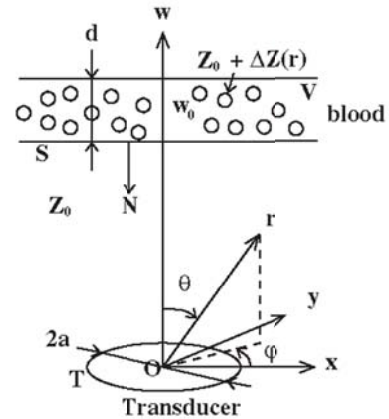


Fig. 2. Illustration of geometrical condition in measurement of echoes from scatterers with a circular transducer.

where  $Z_0$  is the average specific acoustic impedance of the medium. When scatterer diameters are sufficiently smaller than the ultrasonic wavelength [ $k\sigma \ll 1$ ,  $e^{-k^2 \sigma^2} \cong 1$ ,  $S(f) \propto k^4 \sigma^6$ ], echoes from scatterers show Rayleigh behavior, i.e., the power  $S_i(f)$  of scattered waves is proportional to the fourth power of frequency,  $f^4$  [20,22,23]. Echoes from scatterers with

larger diameters include the components of reflection, which have no frequency dependence. Therefore, the spectral slope decreases when the sizes of scatterers increase and the components of reflection are included in the echoes [23].

The measured power spectrum  $P_s(f)$  of the received ultrasonic echo signal  $e_s(t)$  contains both the scattering property  $S_s(f)$  from a microscopic sphere and the frequency responses  $G(f)$  of transmitting and receiving transducers. Therefore, by normalizing the power spectrum  $P_s(f)$  of echoes from scatterers by the power spectrum  $P_r(f)$  from a silicone plate, the frequency responses  $G(f)$  of the transmitting and receiving transducers are removed [25,26].

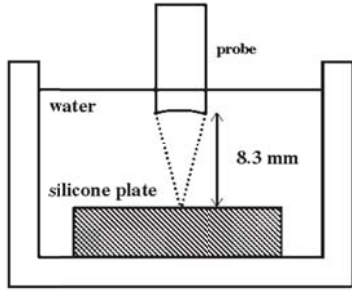


Fig. 3. System for measurement of echoes from the silicone plate.

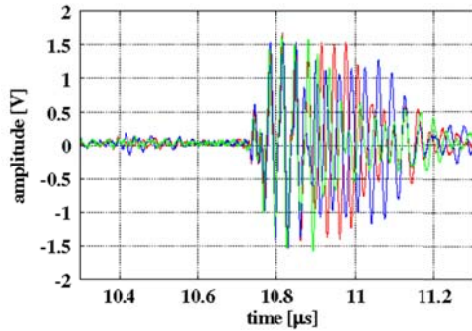


Fig. 4. Three RF echoes from the silicone plate at different points on the surface.

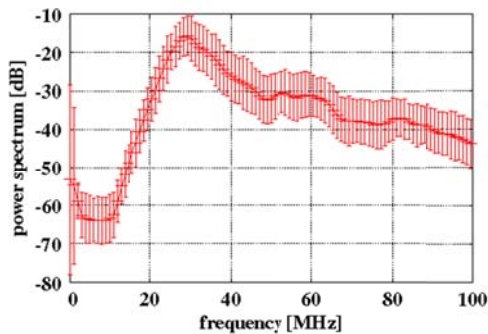


Fig. 5. Means and standard deviations of power spectra of the ultrasound echoes reflected from the silicone plate.

Figure 3 shows a system for measuring an echo  $e_r(t)$  from a silicone plate. The distance between the probe and the silicone plate was equal to that between the probe and the middle part of the intravascular lumen in

an *in vivo* measurement. Figure 4 shows RF echoes reflected by the surface of the silicone plate and scattered from the inside of the silicone plate. Three lines in Fig. 4 show RF signals from different points of the silicone plate. The scatterer distribution in the silicone plate is assumed to be random, and only the echo reflected from the surface can be obtained by averaging the echoes measured at different points on the surface. Therefore, echoes from the silicone plate were acquired at 1000 different points by moving the transducer. In Fig. 4, there are echoes with much smaller amplitudes of around 10.4  $\mu$ s. Such echoes were supposed to be caused by the interference of ultrasonic waves during focusing by the concave transducer used. Such undesirable echoes were suppressed by applying Hanning windows centered at 10.8  $\mu$ s when the Fourier transform was performed. Figure 5 shows the power spectrum  $P_r(f)$  from a silicone plate that was obtained by averaging 1000 power spectra of RF echoes from a number of different points on the surface of the silicone plate. The frequency range used for normalization was limited because the ultrasonic pulse used in this study had a finite frequency bandwidth. In the present study, we estimated the slope of the normalized power spectrum  $P_s(f)/P_r(f)$  using the weighted least-mean-squared method by considering the signal-to-noise ratio (SNR) of the echo at each frequency [27]. Let us define the mean squared difference between the measured spectrum and a linear model as

$$\alpha = \frac{\sum_{i=0}^N e_i^2}{\sum_{i=0}^N w_i^2 [y(f_i) - (ax_i + b)]^2}, \quad (10)$$

where  $y(f_i)$  is the normalized logarithmic power spectrum  $\log_{10}P_s(f)/P_r(f)$  at a frequency of  $f_i$ ,  $x_i$  is the logarithmic frequency  $\log_{10}f_i$ , and  $w_i$  is the weighting function. In this study, the weighting function  $w_i$  was defined by

$$w_i = \frac{P_r(f_i)}{P_{rmax}} \quad (11)$$

where  $P_{rmax}$  is the maximum value of the power spectrum  $P_r(f_i)$  from a silicone plate.

Figure 6 shows the weighting function  $w_i$ . It is assumed that the echoes due to reflection do not show frequency dependence and that only the scattering property of a target remains in the normalized power spectrum  $P_s(f)/P_r(f)$ .

In Rayleigh scattering, the normalized power spectrum  $P_s(f)/P_r(f)$  changes linearly with respect to the logarithmic frequency. In non-Rayleigh scattering, on the other hand, the spectral slope decreases with an increase in scatterer diameter, such an increase being equal to that in the correlation length  $\sigma$  of the Gaussian correlation function. In this study, the diameter of the scatterer was estimated to assess RBC aggregation from the spectral slope by assuming that the correlation length  $\sigma$  of the Gaussian correlation function of

continuous inhomogeneous media corresponds to the diameter of the scatterer.

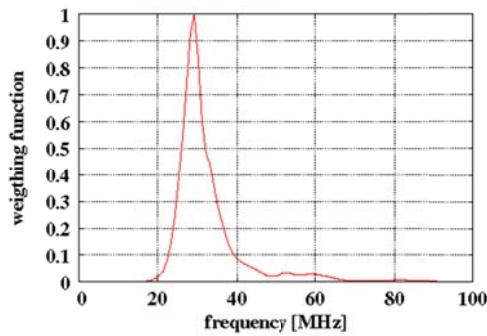


Fig. 6. Weighting function obtained from averaged power spectrum of the ultrasound echoes reflected from the silicone plate.

### 3. Results

#### 3.1. *In vivo* measurements of viscoelasticity of arterial wall

RF data for 2 s obtained by each acquisition included at least an entire cardiac cycle. Therefore, the changes in thickness  $\Delta h(t)$  and blood pressure  $p(t)$  were obtained for at least one cardiac cycle in each measurement for estimating the viscoelastic parameters of the radial arterial wall.

To reveal the change in the stress-strain relationship of the arterial wall due to FMD, the blood pressure  $p(t)$  and the change in the thickness of the intima-media region  $\Delta h(t)$  during a cardiac cycle during FMD were measured. Figure 7 shows the transient change in stress-strain relationship between the change in thickness and the blood pressure of subject A. The stress-strain relationship showed hysteresis property and gradually changed its shape. The slope of the hysteresis loop decreased owing to FMD, which shows that the elastic modulus decreased. In addition to the change in slope, the area of the loop clearly increased after recirculation. The area of the loop depended on the ratio of the loss modulus  $\omega\eta$  ( $\omega$ : angular frequency of strain,  $\eta$ : viscosity) to the static elastic modulus  $E_s$  when the Voigt model was assumed.

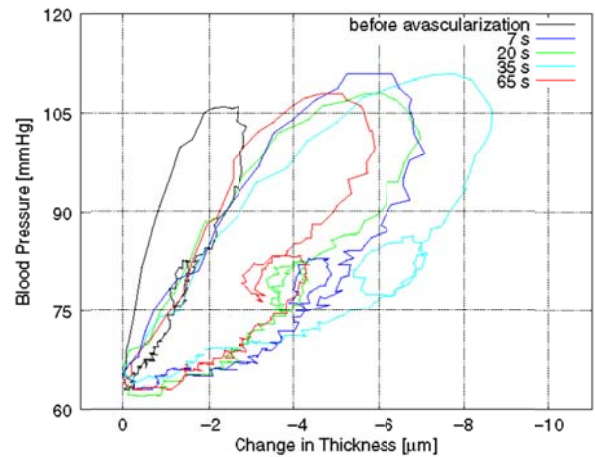


Fig. 7. Transient change in relationship (hysteresis) between blood pressure  $p(t)$  and change in thickness  $\Delta h(t)$  measured in the radial artery *in vivo*.

Figures 8(a) and 8(b) show the time sequence of the blood flow velocities and stress-strain relationships of subject A, respectively. Blood velocity clearly increased immediately after recirculation and the stress-strain relationship started to change. Sixty seconds after recirculation, blood velocity returned to its original value and the stress-strain relationship also came around gradually.

Figure 9(a) shows the transient changes in the means and standard deviations (SDs) of the static elasticity  $E_s$  and viscosity  $\eta$  averaged by 5 ultrasonic beams. These parameters were estimated from the stress-strain relationships obtained from subject A (the first measurement). The transient change in static elasticity  $E_s$  was similar to that in a different elastic parameter reported in the literature [5]. The minimum static elasticity  $E_s$  was measured at 35 s after the release of the cuff. The maximum percentage change in static elasticity  $E_s$  was about 57% (770 kPa). Moreover, the viscosity  $\eta$ , which was evaluated noninvasively by the proposed method, increased after recirculation. The measured viscosity was in the same range as the viscosity at the carotid artery reported in the literature (*in vitro* measurement) [28]. The maximum viscosity  $\eta$  at 35 s after recirculation was about 21 kPa·s, which was about 94% (10 kPa·s) larger than the mean at rest.

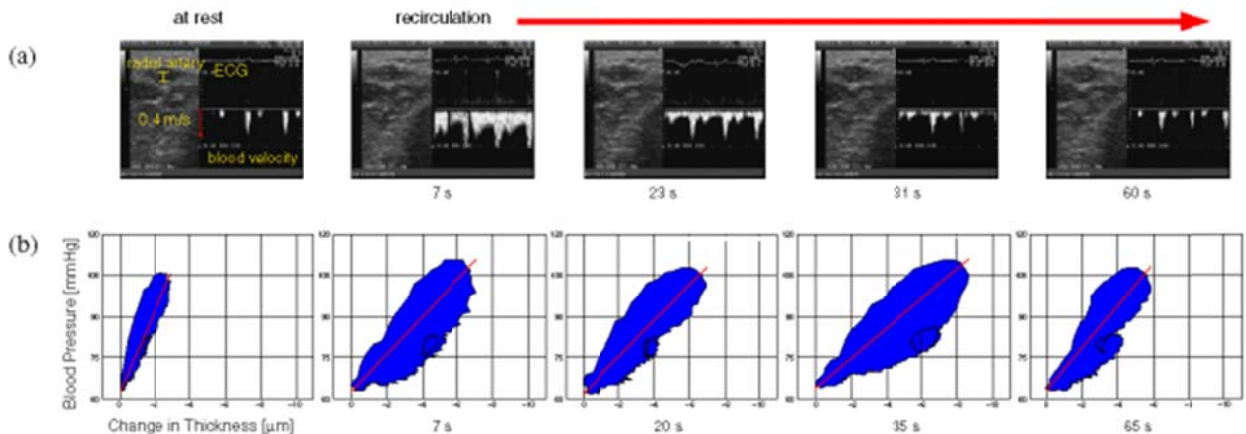


Figure 9. (a) Time sequence of blood flow velocity measurements and (b) stress-strain relationship (hysteresis) (b).

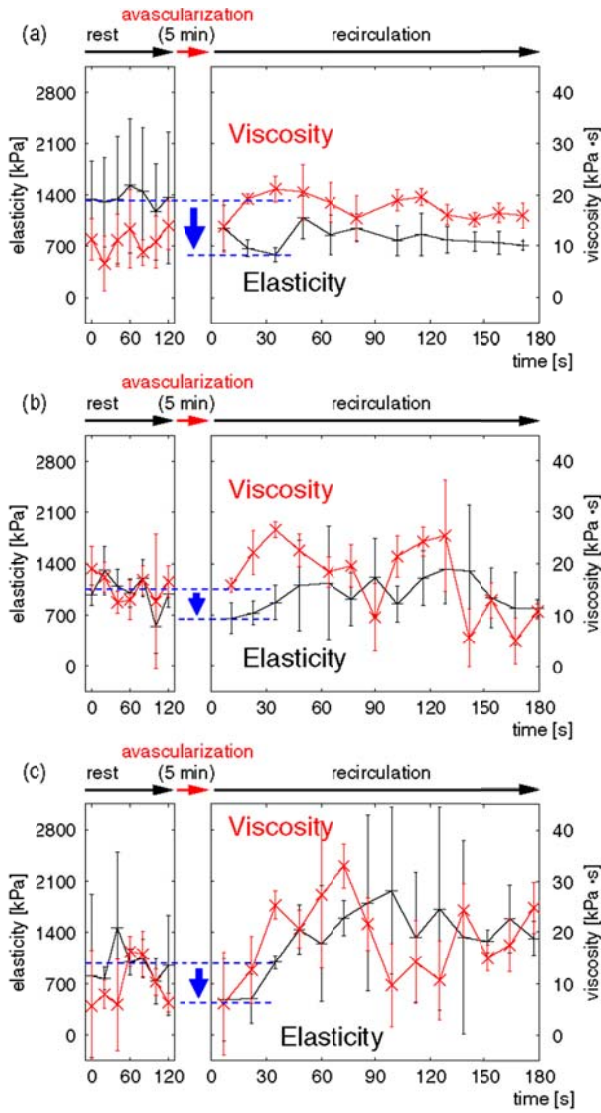


Fig. 9. Transient change in means and SDs of estimated static elasticity  $E_s$  and viscosity  $\eta$  measured in subject A: (a) first, (b) second, and (c) third measurements.

Figures 9(b) and 9(c) show the transient changes in the means and SDs of the static elasticity  $E_s$  and viscosity  $\eta$  measured in the same subject on other days (the second and third measurements in subject A). The maximum percentage change in static elasticity  $E_s$  observed at 11 s after recirculation was about 36% (360 kPa) in the second measurement, and that at 7 s after recirculation was about 50% (490 kPa) in the third measurement. The maximum increase in viscosity at 35 s after recirculation was about 73% (11 kPa·s) in the second measurement and that at 73 s after recirculation was about 240% (23 kPa·s) in the third measurement from the means at rest.

Figure 10 shows the transient change in the means and SDs of the static elasticity  $E_s$  and viscosity  $\eta$  measured in another subject (subject B). The maximum percentage change in static elasticity  $E_s$  at 19 s after recirculation was about 55% (570 kPa). The maximum increase in viscosity  $\eta$  at 44 s after recirculation was about 571% (23 kPa·s) from the mean at rest. The

temporal decrease in elasticity  $E_s$  and the increase in viscosity  $\eta$  were observed also in another subject.

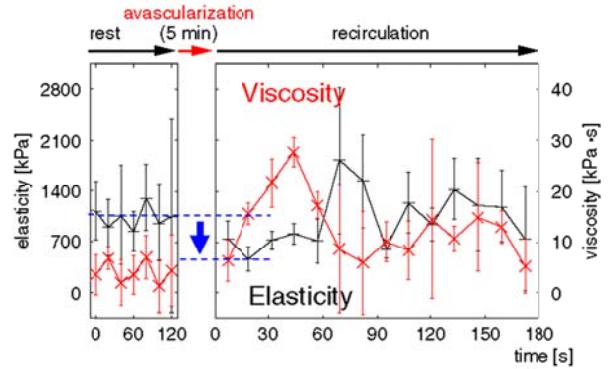


Fig. 10. Transient change in means and SDs of estimated static elasticity  $E_s$  and viscosity  $\eta$  measured in another subject (subject B).

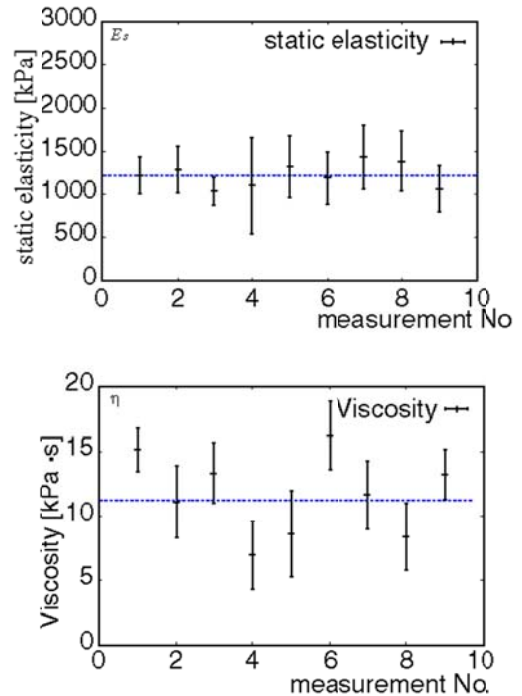


Fig. 11. Means and SDs of static elasticity  $E_s$  and viscosity  $\eta$  for 10 min *in vivo* measurements.

	Static elasticity $E_s$ (kPa)	Viscosity $\eta$ (kPa·s)
Average	1225.1	11.6
SD	640.1	5.0

Table I. Means and SDs of parameters for 10 min *in vivo* measurements.

For the evaluation of reproducibility, RF data and the blood pressure waveform at rest were measured every 1 min for 10 min. Figure 11 shows the means and SDs of the measured static elasticity  $E_s$  and viscosity  $\eta$ . The SDs were obtained from 30 ultrasonic beams. Horizontal dashed lines show the means of the parameters.

Figure 11 shows the means and SDs of the parameters. Table I shows the means and SDs of the

parameters averaged for 10 min. For the static elasticity  $E_s$ , the maximum difference from the mean was about 200 kPa (17% of mean). The maximum change in static elasticity due to FMD (770, 360, 490, and 570 kPa) was much larger than this value. For the viscosity  $\eta$ , the variation in mean was 5 kPa·s. The maximum change in viscosity due to FMD (10, 11, 23, and 23 kPa·s) was also much larger than this value. However, the patterns of the changes in the static elasticity  $E_s$  and viscosity  $\eta$  after recirculation, and the time for observing the maximal changes in these parameters were different among these measurements.

### 3.2 Evaluation of red blood cell aggregation

#### 3.2.1 Basic experiments using microspheres

The ultrasound diagnostic equipment (Tomey UD-1000) employed is equipped with a mechanical scan probe at a center frequency  $f_0$  of 40MHz (wavelength is about 40  $\mu\text{m}$ ). RF echoes were acquired at a sampling frequency of 1 GHz at a 16-bit resolution by the oscilloscope (Tektronix DPO7054), and their power spectra  $\{P(f)\}$  were obtained by Fourier transform with a Hanning window of 1.024  $\mu\text{s}$  length. To reduce the effect of random noise, 1000 power spectra were averaged. The left-hand column of Table II shows the different diameters of measured microspheres. Microspheres (1) and (3) were made of copolymer with  $\text{Cl}_2$ , and microspheres (2) and (4) were made of copolymer without  $\text{Cl}_2$ . Microspheres with different diameters, which were mixed with water at a concentration of 3.00 g/l, simulated nonaggregated and aggregated RBCs. This concentration is lower than that of RBCs in actual blood, preventing the aggregation of microspheres. RF echoes from the spheres around the focal point were acquired from spatially different regions by mechanical linear scan as in the measurement of a silicone plate to acquire many statistically independent data points. Effects of the difference between acoustic impedances of microspheres and RBCs were not considered in the present study, although such effects should be investigated in future studies.

	Particle diameter ( $\mu\text{m}$ )	Slope ( $1/\log_{10} f$ )	Intercept (dimensionless)
(1)	$5 \pm 2$	3.46	-27.2
(2)	$11 \pm 3$	1.78	-14.8
(3)	$15 \pm 5$	1.47	-12.9
(4)	$30 \pm 10$	0.02	-0.56

Table II. Microsphere diameters and experimental results.

Figure 12(a) shows the averaged power spectra of echoes from the microspheres, and Fig. 12(b) shows the normalized power spectra. The numbers correspond to the microsphere numbers in Table II. The spectral slope and intercept values are shown in the right-hand column of Table II. Figure 13 shows the mean and standard deviation of spectral slopes for ten measurements of each microsphere. In Fig. 12, the slope of the normalized power spectrum  $P_s(f)/P_r(f)$  of a

larger scatterer is smaller than that of a smaller scatterer. This result shows that the slope of the normalized logarithmic power spectrum  $\log_{10} P_s(f)/P_r(f)$  is related to the diameter of the scatterer.

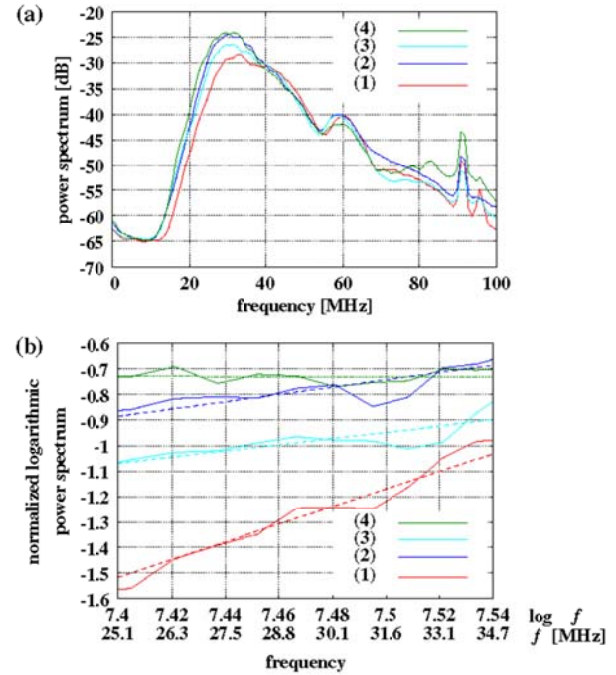


Fig. 12. (a) Averaged power spectra of the ultrasonic echoes scattered from microspheres of various sizes and (b) normalized power spectra and the weighted least-mean-squared regression lines of microspheres (1)–(4) in Table II.

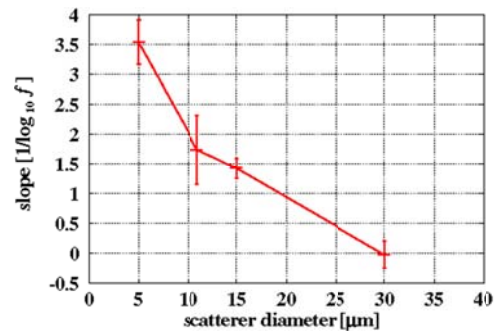


Fig. 13. Mean and the standard deviation of the estimated spectral slopes as a function of scatterer diameter.

#### 3.2.2 In vivo experiments

The main components of normal blood are RBCs, which do not aggregate in large veins because of blood flow [29,30]. To measure ultrasonic echoes from aggregated RBCs in addition to those from nonaggregated RBCs, blood flow was stopped by pressurizing a cuff surrounding the upper arm at 250 mmHg. Ultrasonic echoes were acquired at rest for 2 min, during avascularization for 5 min, and after recirculation for 3 min. Figure 14 shows B-mode images of a vein at the dorsum manus of a 24-year-old healthy male. B-mode images were measured at rest (1), at the beginning of avascularization (2), at the end of

avascularization (3), at the beginning of recirculation (4), and 120 s after recirculation (5). It is possible to reduce the attenuation of high frequency ultrasound because the vein at the dorsum manus is a superficial blood vessel. The vein measured in this study had a large diameter and a high steady blood flow rate, which affect RBC aggregation, and thus, the measurement could be assumed to be performed with respect to the nonaggregated RBCs at rest. In addition, we measured the change in spectral slope caused by the change in blood flow rate due to avascularization using a cuff. RF echoes from the focal point positioned in the vessel lumen were acquired from many different positions by mechanical linear scan to reduce the effect of the increase in scatterer diameter variation due to aggregation.

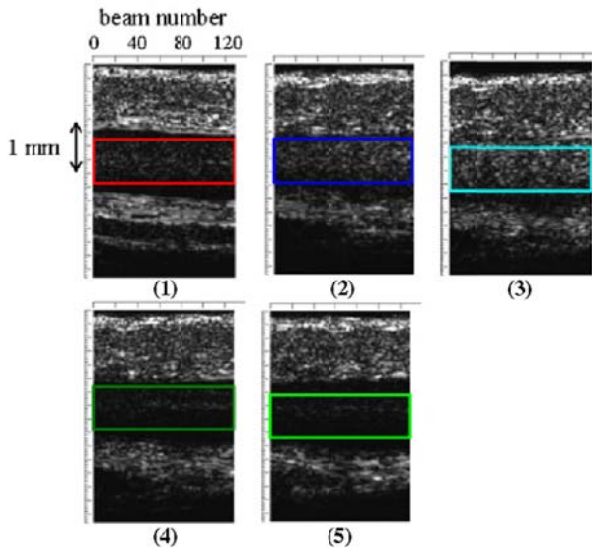


Fig. 14. B-mode images and windows of the vein at the dorsum manus: (1) at rest, (2) at the beginning of avascularization, (3) at the end of avascularization, (4) at the beginning of recirculation, and (5) 120 s after recirculation.

Figure 15 shows the normalized logarithmic power spectrum  $\log_{10}P_s(f)/P_r(f)$  obtained from the lumen of the vein at the dorsum manus of the 24-year-old healthy male and the weighted least-mean-squared regression line. Figure 16 shows the transient change in estimated spectral slope due to avascularization. The slope of the normalized power spectrum of echoes from RBCs at rest was close to that of microsphere (3) (diameter: 15  $\mu\text{m}$ ) in Table II. The RBC diameter is 8  $\mu\text{m}$  at most and this diameter is between those of microspheres (1) (diameter: 5  $\mu\text{m}$ ) and (2) (diameter: 11  $\mu\text{m}$ ). The spectral slope measured for RBCs was slightly greater than that of a sphere whose diameter corresponds to that of an RBC. One of the reasons for this was considered to be the frequency dependent attenuation of ultrasound during propagation in biological tissues. If the attenuation coefficient and the depth to vein are assumed to be 1 dB  $\cdot$  MHz $^{-1}$   $\cdot$  cm $^{-1}$  and 1 mm, respectively, the differences between two logarithmic normalized power spectra  $\log_{10}P_s(f)/P_r(f)$  with and without attenuation are 5 dB at 25 MHz and 7

dB at 35 MHz. Accordingly, the spectral slope decreases by 1.37 in the frequency band of 25-35 MHz. Therefore, the measured spectral slope of RBCs was shown to be decreased.

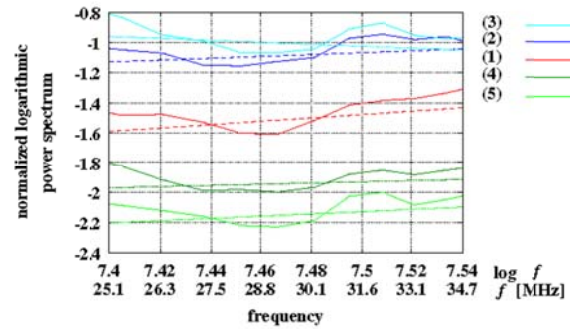


Fig. 15. Normalized power spectra and the least-mean-squared regression lines.

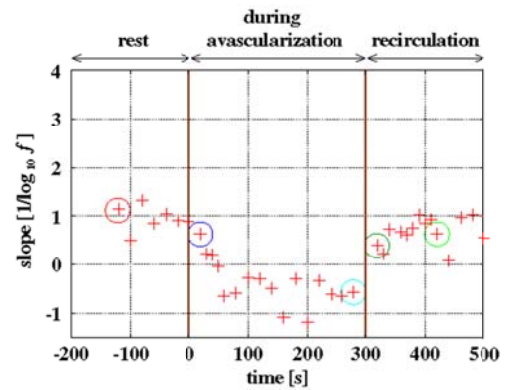


Fig. 16. Transient change in the estimated spectral slope during avascularization for 5 min.

Furthermore, the spectral slope gradually decreased during avascularization and returned to the levels of rest in the *in vivo* measurement. Although there are still many factors to be investigated, such as acoustic impedances of microspheres, methods for normalization, and calibration of the system [30], these results showed that the slope of the normalized power spectrum changes with scatterer diameter.

## 5. Conclusion

In this study, methods for measurement of viscoelasticity of arterial wall and evaluation of red blood cell aggregation were developed. Such methods would be useful for early diagnosis of atherosclerosis.

## Acknowledgments

We would like to thank Tomey Corporation for its cooperation on the use of the diagnostic equipment.

## References

[1] Ross R. Atherosclerosis – An inflammatory disease. *N Engl J Med* **340**, 115-126, 1996.

- [2] Matsuzawa Y. *Jpn J Clin Med* **51**, 1951–1953, 1993 [in Japanese].
- [3] Yamamoto M and Yamamoto K. *Jpn J Clin Med* **51**, 1980–1986, 1993.
- [4] Corretti MC, Anderson TJ, Benfamin EJ, Celermajer D, Charbonneau F, Creager MA, Deanfield J, Drexler H, Gehard-Herman M, Herrington D, Vallance P, Vita J and Vogel R. Guidelines for the ultrasound assessment of endothelial-dependent flow-mediated vasodilation of the brachial artery. *J Am Coll Cardiol* **39**, 257–267, 2002.
- [5] Kaneko T, Hasegawa H and Kanai H. Ultrasonic measurement of endothelium-dependent relaxation response by high accuracy detection of arterial wall boundary. *Jpn J Appl Phys* **48**, 4881–4888, 2007.
- [6] Pyke KE and Tschakovsky. The relationship between shear stress and flow-mediated dilation: Implications for the assessment of endothelial function. *J Physiol* **568**, 357–369, 2005.
- [7] Kanai H, Sato M, Koiwa Y and Chubachi N. Transcutaneous measurement and spectrum analysis of heart wall vibrations. *IEEE Trans Ultrason Ferroelectr Freq Contr* **43**, 791–810, 1996.
- [8] Ikeshita K, Hasegawa H and Kanai H. Ultrasonic measurement of transient change in the stress-strain property of radial arterial wall caused by endothelial-dependent vasodilation. *Jpn J Appl Phys* **47**, 4165–4169, 2008.
- [9] Ikeshita K, Hasegawa H and Kanai H. Flow-mediated change in viscoelastic property of radial arterial wall measured by 22-MHz ultrasound. *Jpn J Appl Phys* **48**, 07GJ10-1–07GJ10-5, 2009.
- [10] Tsuzuki K, Hasegawa H, Kanai H, Ichiki M and Tezuka F. Threshold setting for likelihood function for elasticity-based tissue classification of arterial wall by evaluating variance in measurement of radial strain. *Jpn J Appl Phys* **47**, 4180–4187, 2008.
- [11] Ujiie K. *Silent Clots: Life's Biggest Killers*. Chuo Art Publishing, Tokyo, 2000.
- [12] Vander AJ, Sherman JH and Luciano DS. *Human Physiology: The Mechanisms of Body Function*. McGraw-Hill, Boston, 1998.
- [13] Paeng DG, Chiao RY and Shung KK. Echogenicity variations from porcine blood II: The 'bright ring' under oscillatory flow. *Ultrasound Med Biol* **30**, 815–825, 2004.
- [14] Amararenea A, Gennisson, Rabhi A and Cloutier G. Quantification of red blood cell aggregation using an ultrasound clinical imaging system. *IEEE Ultrason. Symp.* 874–877, 2005.
- [15] Alt E, Banyai S, Banyai M and Koppensteinerr R. Blood rheology in deep venous thrombosis: Relation to persistent and transient risk factors. *Thromb Res* **107**, 101–107, 2002.
- [16] Lee AJ, Mowwbray PI, Lowe GDO, Rumley A, Fowkes FGR and Allan PL. Blood viscosity and elevated carotid intima-media thickness in men and women. The Edinburgh artery study. *Circulation* **97**, 1467–1473, 1998.
- [17] Huang CC and Wang SH. Characterization of blood properties from coagulating blood of different hematocrits using ultrasonic backscatter and attenuation. *Jpn J Appl Phys* **45**, 7191–7196, 2006.
- [18] Kikuchi Y, Sato K and Mizuguchi Y. Modified cell-flow microchannels in a single-crystal silicone substrate and flow behavior of blood cells. *Microvasc. Res* **47**, 126–139, 1994.
- [19] Saitoh N, Hasegawa H and Kanai H. Estimation of scatterer diameter using ultrasonic backscattering property for assessment of red blood cell aggregation. *Jpn J Appl Phys* **48**, 07GJ08-1–07GJ08-5, 2009.
- [20] Ueda M and Ozawa Y. Spectral analysis of echoes for backscattering coefficient measurement. *J Acoust Soc Am* **77**, 38–47, 1985.
- [21] Yagi S and Nakayama K. Acoustic scattering in weekly inhomogeneous dispersive media: Theoretical analysis. *Acoust Soc Jpn* **36**, 496–503, 1980.
- [22] Insana MF, Wagner RF, Brown DG and Hall TJ. Describing small-scale structure in random media using pulse-echo ultrasound. *J Acoust Soc Am* **87**, 179–192, 1990.
- [23] Yua FHT and Cloutier G. Experimental ultrasound characterization of red blood cell aggregation using the structure factor size estimator. *J Acoust Soc Am* **122**, 645–656, 2007.
- [24] Fontaine I and Cloutier G. Modeling the frequency dependence (5–120 MHz) of ultrasound backscattering by red blood cell aggregates in shear flow at a normal hematocrit. *J Acoust Soc Am* **113**, 2893–2900, 2003.
- [25] Lizzi FL, Greenebaum M, Feleppa EJ, Elbaurn M and Coleman DJ. Theoretical framework for spectrum analysis in ultrasonic tissue characterization. *J Acoust Soc Am* **73**, 1366–1373, 1983.
- [26] Lizzi FL, Astor M, Kalisz A, Liu T, Coleman DJ, Silverman R, Ursea R and Rondeau M. Ultrasonic spectrum analysis for assay of different scatterer morphologies: Theory and very-high frequency clinical results. *IEEE Ultrason Symp*, 1155–1159, 1996.
- [27] Kanai H. *Spectrum Analysis of Sound and Vibration*, Corona Publishing, Tokyo, 1999.
- [28] Learoyd BM and Taylor MG. Alterations with age in the viscoelastic properties of human arterial walls. *Circ Res* **18**, 278–292, 1966.
- [29] Yagi S and Nakayama K. Acoustic scattering in weakly inhomogeneous dispersive media: Experimental analysis. *Acoust Soc Jpn* **39**, 659–667, 1983.
- [30] Yagi S and Nakayama K. Absolute measurement of scattering characteristics of dispersive media using ultrasonic wideband pulse. *Acoust Soc Jpn* **43**, 777–785, 1987.